ELSEVIER

Nuclear Instruments and Methods in Physics Research B 124 (1997) 225–231

NIM B
Beam Interactions
with Materials & Atoms

Kinematically complete experiments using cold target recoil ion momentum spectroscopy

R. Dörner [a,*], V. Mergel [a], L. Spielberger [a], M. Achler [a], Kh. Khayyat [a], T. Vogt [a], H. Bräuning [a], O. Jagutzki [a], T. Weber [a], J. Ullrich [b], R. Moshammer [a], M. Unverzagt [a], W. Schmitt [b], H. Khemliche [c], M.H. Prior [c], C.L. Cocke [d], J. Feagin [e], R.E. Olson [f], H. Schmidt-Böcking [a]

[a] *Institut für Kernphysik, Universität Frankfurt, August Euler Str. 6, D60486 Frankfurt, Germany*
[b] *Gesellschaft für Schwerionen Forschung, D64291 Darmstadt, Germany*
[c] *LBNL, Berkeley, CA 94720, USA*
[d] *Department of Physics, Kansas State University, Manhattan, KS 66506, USA*
[e] *Department of Physics, California State University-Fullerton, Fullerton, CA 92634, USA*
[f] *Department of Physics, University of Missouri, Rolla, MS 65401, USA*

Abstract

Cold Target Recoil Ion Momentum Spectroscopy allows the detection of the three-dimensional momentum vector of the recoiling product ion from ion, electron or photon atom collisions with 4π solid angle and high resolution. It can be combined with large area position-sensitive detectors for electron detection or measurement of the projectile charge-state and scattering angle. Such 'reaction microscopes' cover the full correlated momentum space of all fragments of an atomic reaction yielding kinematically complete information for each reaction event. For the first time in atomic collision physics fully differential data became available in the sense that not only the momenta of all fragments, but also the complete momentum space is observed in one experiment. Recent results achieved with this new technique for slow p–He collisions and threshold photo ionization of He will be discussed.

1. Outline of COLTRIMS

With the development of new experimental techniques which exploit large area position-sensitive detectors and time-of-flight measurements for the coincident detection of the reaction products of an atomic collision, it recently has become possible to perform fully differential experiments. Such experiments result in kinematically complete information on the reaction under investigation. They yield multidimensional images of the square of the correlated final state wavefunction and the most complete and detailed information achievable for a continuum state if one neglects the spin. Recoil-ion momentum spectroscopy is the key technology in this rapid development. It allows determination of the charge-state and the three-dimensional momentum vector of the ions of an atomic reaction with a unique combination of high resolution and 4π solid angle. In addition to the momentum of the ion from the reaction, other products like electrons or a scattered projectile can be analysed with respect to their momentum. The data obtained by this technique are fully differential in a double sense. First, for each reaction event the momenta of all particles in the final state are measured. Second, the full momentum space of all particles is covered in one experiment. In this respect such a fully-differential study includes all experiments on the particular reaction. That is in the offline analysis of the data any question concerning the final momentum states can be answered without performing a new experiment. To achieve kinematically complete information one needs to measure $3n-4$ momenta in the final state, where n is the number of particles in the continuum. The remaining 4 momenta can than be calculated from energy and momentum conservation.

For reactions with only two particles in the final state, like photo single ionization or electron capture, already the recoil-ion momentum alone gives complete information on the process. Single ionization by absorbtion of one photon is a particular simple example.

Momentum conservation requires that in the final state

---

[*] Corresponding author. email: doerner@ikf007.ikf.physik.uni-frankfurt.de.

PII S0168-583X(96)00877-4

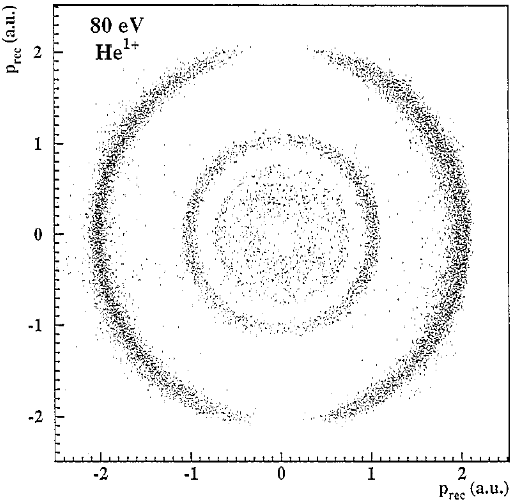

Fig. 1. Momentum distribution of He^{1+} ions created by 80 eV linear polarized photons. The polarization axis and the electric extraction field for the ion detection is along the x-direction. The data are integrated over a momentum rang of ± 0.1 a.u. in the z directions. The outer circle results from ions in the ground state, the inner circles are progressive higher excited states.

the sum of the electron and the recoil-ion momentum add up to the photon momentum, which is only 0.03 a.u. at $E_\gamma = 100$ eV. Thus the recoil ion momentum measurement is equivalent to detection of the electron [1,2]. Fig. 1 shows the He^{1+} momentum distribution after absorption of a 80 eV photon. The outer ring corresponds to ions in the ground state, where the electron has an energy of $80 - 24.6 = 55.4$ eV. The inner rings result from ions in excited states. The ion carries momentum opposite to the electron but due to the mass difference, energy and angular momentum are mainly in the electronic motion. This information in the ion momentum has been used to measure new precise data for the ratio of double- to single-ionization from 80–400 eV [1] and to separate photoabsorption from the Compton scattering [2].

A second example with only two particles in the final state are electron capture reactions. For this process any change of the projectile momentum must be mirrored in the recoiling target-ion momentum. Thus recoil-ion momentum spectroscopy is, in this case, equivalent to translational spectroscopy. The transverse momentum of the recoil ion reflects the projectile scattering angle and the recoil-ion longitudinal momentum gives the energy gain (or loss) of the projectile, hence the information on the Q-value of the reaction. In a direct measurement of the projectile ion scattering one has to observe a small change on a large momentum vector, which restricts this technique to low impact energies. If one observes the momentum exchange via the recoil ion one is not restricted in the choice of impact energies and projectile masses. Recoil-ion momentum spectroscopy thus allows high resolution energy gain measurements which simultaneously give the information on the scattering angle distribution even for fast and heavy projectiles [3–6]. For example, Mergel and cooworkers [4,5] reported a resolution of $\Delta E/E = 10^{-5}$ for 0.25 MeV He^{2+} + He collisions.

For reactions with more than two particles in the final state a complete experiment is much more challenging. For example, in the long studied process of electron impact single ionization, 5 momentum components of the three particles need to be measured. Traditionally this has been achieved by coincident detection of two electrons. Such (e, 2e) experiments are complete in the first sense that they measure all momenta of the fragments at the energy and angular setting of the detectors. However, an infinite number of combinations of energies and angles between the electrons would have to be measured to yield complete information in the second sense, of covering the full final state. Using recoil ion momentums spectroscopy this can by achieved by detection of the ion and one of the electrons. For electron impact single ionization and photon impact double ionization in principal the detection of all electrons ((e, 2e) and (γ, 2e)) is equivalent to detecting the ion and neglecting one of the electrons. However, the experimental setup discussed below which measures the momentum of the ion and one of the electrons reaches 4π solid angle for both and thus a coincidence efficiency orders of magnitude higher than traditional coincident electron spectroscopy.

For ion impact single ionization a complete experiment requires meaurement of the momenta of two of the three final state particles (electron, scattered projectile and recoil ion). One can for example measure the azimuthal and polar scattering angle of the projectile in coincidence with either the electron [7] or the recoiling ion [8–10]. For fast heavy ion impact, however, it is impossible to detect the momentum change of the heavy projectile with sufficient resolution. For such collision systems the coincident detection of the electron and the recoil ion is the only feasible way to make a complete experiment [17,19,20].

We will first give a short description of the technique of recoil ion momentum spectroscopy and then discuss two recent complete experiments performed with this technique. One on single ionization of He by slow p impact and a second one on double photoionization of He.

2. Experiment

The basic idea for high resolution 4π spectrometers is identical for ion and electron detection. They are based on a small reaction volume from which the fragments are guided by electric and magnetic fields to large area position-sensitive detectors. The momenta of electron and ion can than be calculated from the time-of-flight and the position where the particles hit the detector. The momentum measurement for the ion is complicated by the fact that the typical momenta in atomic reactions are in the order of the thermal motion of the target, which is 4.6 a.u. (atomic units) for He atoms at room temperature. Thus, one has to provide an internally cold atomic target for the collision. This is presently achieved by using supersonic gas-jet targets. A further improvement in resolution is envisaged by the future use of laser cooled targets.

In the experiments presented below a precooled supersonic gas jet has been used. A gas reservoir was mounted on a cryogenic cold head to cool the He gas to 15–30 K before it expands through a 30 μm hole. From this expansion a supersonic jet is formed and the He atoms have a mean speed proportional to the square root of the nozzle temperature. The momentum distribution around the mean value is given by the speed ratio of the expansion [11]. The precooling helps to achieve a narrow momentum distribution with small turbo pumps. About 1 cm above the nozzle, the inner part of the preformed gas jet enters the scattering chamber through a skimmer of 0.3 mm diameter. In the present jet a driving pressure of 400 mbar has been used. It resulted in 5×10^{-4} mbar in the source chamber and a local target pressure of a few 10^{-5} mbar at the target region, 3 cm above the skimmer. The gas jet leaves the scattering chamber into a separately pumped jet

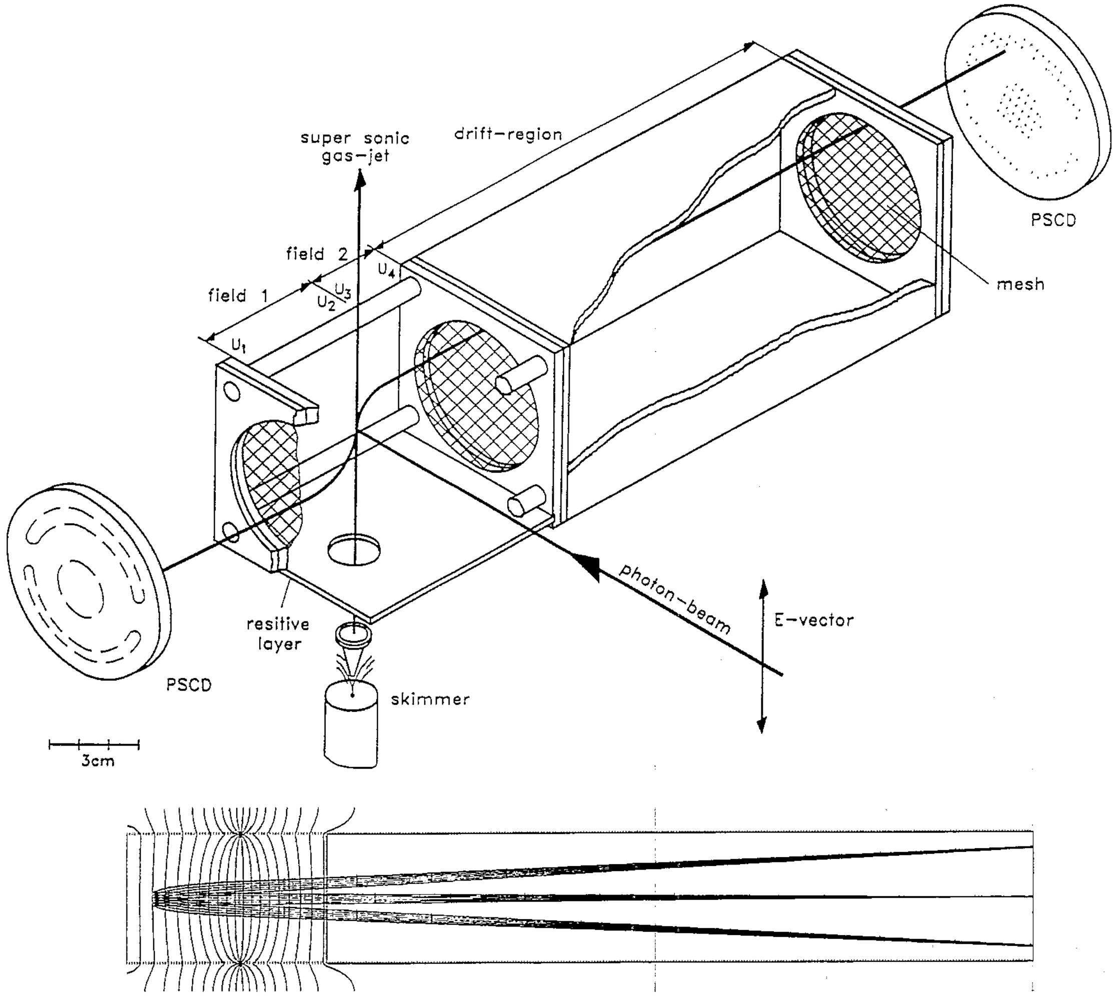

Fig. 2. Recoil ion momentum spectrometer as used for the two experiments discussed in this paper. The gas nozzle is cooled to 15–30 K, the supersonic gas jet has a diameter of 1.1 mm at the intersection with the projectile beam. The field configuration for the ion branch is shown in the lower part of the figure. The electron detector is located on the left side of the spectrometer and the ion detector on the right side. The three different sets of rays correspond to ions with different starting momenta, the lines within one band to different starting positions. The field geometry with the lens has been optimized so that different starting positions lead to the same position on the channel plate and to the same time of flight (three-dimensional focussing) (from Ref. [10]).

dump. Source chamber, scattering chamber and jet dump are each pumped by 220 l/s turbo molecular pumps.

The ions are created in the overlap volume of the gas jet with the projectile beam. Different designs for recoil ion and electron spectrometers have been used. In a first version a homogeneous electric field followed by a drift tube guided the ions to a position sensitive channel plate [12,4,13–16]. With this homogenous field spectrometer Mergel and coworkers [4] reported a resolution of 0.26 a.u. A very flexible combination of electric fields for ion detection and magnetic field for guiding of electrons has been used by a group at GSI [17–19]. Their 'momentum microscope' is discussed in detail in Ref. [20]. In all spectrometers with homogeneous fields the ion momentum resolution is restricted by the extension of overlap volume. To circumvent this restriction Mergel [10] has designed a field geometry which is focusing in three dimensions (see Fig. 2). An electrostatic lens in the extraction region focuses different starting positions perpendicular to the extraction field onto one point on the detector. As can be seen in Fig. 2 this can be achieved without loosing the information on the starting momentum. Also in the third direction different starting points along the field lead to the same time-of-flight. Thus, high resolution can be achieved even with a gas target extended over several mm. With this spectrometer a resolution of 0.07 a.u. FWHM, which is close to the internal temperature of the gas jet, has been reached [21]. With the improved properties of such focusing spectrometers another restriction for the resolution becomes observable. In front of the position-sensitive channel plate woven meshes have to be used to shield the post-acceleration field towards the channel-plate surface from the field free drift tube. The finite mesh width of those grids restricts the achievable position resolution. A spectrometer which avoids all of the grids is in preparation.

Due to the low energy of the recoiling ions a moderate field of a few V/cm is sufficient to collect all ions onto the detector. The same field is used to guide the electrons in the opposite direction. If one chooses a distance of 2 cm from the target region to the electron detector a 4π collection efficiency can be reached only for very low energy electrons (1–5 eV). In the two experiments reported below such low energy electrons were dominant. In fast particle collisions, however, higher energy electrons are created. To guide such electrons to the detector, Moshammer and coworkers [20], have superimposed on the electric field a homogenous magnetic field yielding 4π detection efficiency up to 30 eV electron energy. Higher electron energies can be accessed by increasing the magnetic and electric fields.

To measure all three momentum components of electron and ion a reference signal for the time-of-flight measurement is required. This can either be achieved by detecting the projectile in coincidence [17] or by using a pulsed beam [22]. The latter was the case in the photo ionization experiment reported below. For the p–He collision system the electron momentum in the field direction was so small that one could assume a constant time-of-flight for all electrons with good approximation and no time-of-flight measurement for the electrons was performed at all [23,24].

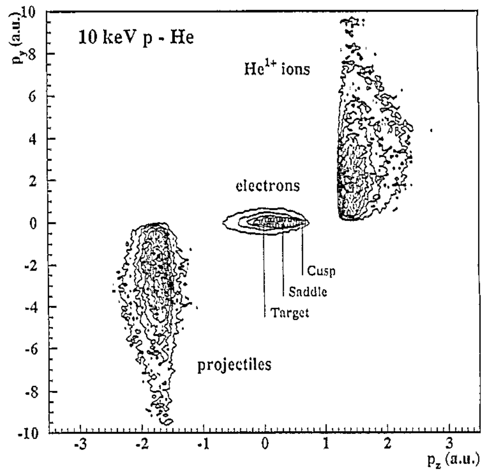

Fig. 3. Distribution of momentum exchanges to the projectile, electron and recoil ion for the reaction 10 keV $p + \mathrm{He} \rightarrow p + \mathrm{He}^{1+} + e^-$. The projectile moves from left to right, the y-axis is defined by the transverse momentum of the recoil ion. The ion and electron momenta have been measured, the projectile momentum has been calculated using momentum conservation for each event. A more detailed view of the electron distribution for fixed momenta of the ion can be found in [23] and the contribution of Pieksma et al. in this volume.

3. Three-body momentum exchange in slow p–He collisions

For atomic collisions where the projectile velocity is smaller or on the order of the orbital velocity of the target electron, capture to bound states of the projectile is the most probable process to ionize the target. For the case where the electron is emitted into the continuum, Fig. 3 shows the distribution of momentum transfers to the three particles in the final state (10 keV $p + \mathrm{He} \rightarrow p + \mathrm{He}^{1+} + e^-$). The z direction is defined by the beam direction (projectile moving from left to right), the y-axis was chosen to be the transverse direction of the recoiling ion. The momenta of electron and ion have been measured in coincidence, the change in projectile momentum has been calculated exploiting momentum conservation. One observes large momentum transfers between projectile and ion and only small momenta of the electron. The momentum transfer to the projectile is backward directed since the reaction is endothermic, i.e. the projectile looses energy and thus momentum. The minimum energy transfer for this reaction channel is given by the binding energy of the target and corresponds to a momentum transfer of -1.44 a.u.. The momentum of the recoil ion is strongly forward-directed. This is in contrast to the situation at fast p–He collisions. At 0.5 MeV impact energy Dörner and coworkers [15] found the recoil longitudinal momentum to be centered around zero in agreement with CTMC calculations, and continuum distorted wave calculations [25]. For Ni^{24+} on He collision Moshammer and coworkers [17] found even a backward emission of the recoil ions due to post collision interaction. In the slow collision discussed here the forward recoil ion momentum results from momentum conservation. One can easily show that the minimum longitudinal recoil momentum which is allowed is associated with emission of a cusp electron and is 1.1 a.u. for the present case [25]. In terms of mechanism this forward recoil emission can be understood from the quasi-molecular nature of the slow collision process. During the collision, for a short time a molecule is formed in which the electron glues the target nucleus to the forward moving projectile leading to a momentum transfer in forward direction. As the quasi molecule breaks up, in most cases the electron is retained by either the target or the projectile leading to electron capture, which is not shown in Fig. 3. For the few cases where the electron is 'stranded' in the continuum [26] it thus is mainly found between the two centers of target and projectile. An electron in the target continuum would appear at momentum zero in the plot while at 10 keV the projectile continuum is located at $p_z = 0.63$ a.u.. The maximum of the electron distribution is found in between these two values. The saddle point of the potential between the projectile and target ions is located at 0.315 a.u..

As is obvious from Fig. 4 the electron plays almost no role in the transverse momentum balance. Projectile and recoil ion compensate their transverse momenta resulting from their internuclear repulsion. The plane shown in Fig. 3 is defined by the recoil ion momentum and the projectile incoming momentum. One finds that the final projectile momentum is mostly in this plane. This is in contrast to the situation for fast collisions. For 3.6 MeV/u Ni^{24+} on He collisions, for example Moshammer and coworkers, have shown that the transverse momentum of the projectile is small and the ion and electron compensate their momenta (similar to the situation in photo ionization). For 0.5–3 MeV p impact Dörner and coworkers [8] and Gensmantel and coworkers [9] showed that in an intermediate range of scattering angles a binary encounter between projectile and electron dominate over the momentum exchange between the two heavy partners.

The single events of the distributions shown in Fig. 3 are measured in coincidence (which allows fixing the plane) but are than integrated over the momenta of the other particles. The experiment, however, gives much more information since for each event the momenta of all three particles are known. This allows, for example, determination of the electron momentum distribution for fixed transverse momentum of projectile or recoil ion both in and out of the plane shown in Fig. 3. Such a detailed analysis of for 5–15 keV p–He collisions can be found in [22] and some results are shown in the contribution by Pieksma in these Proceedings.

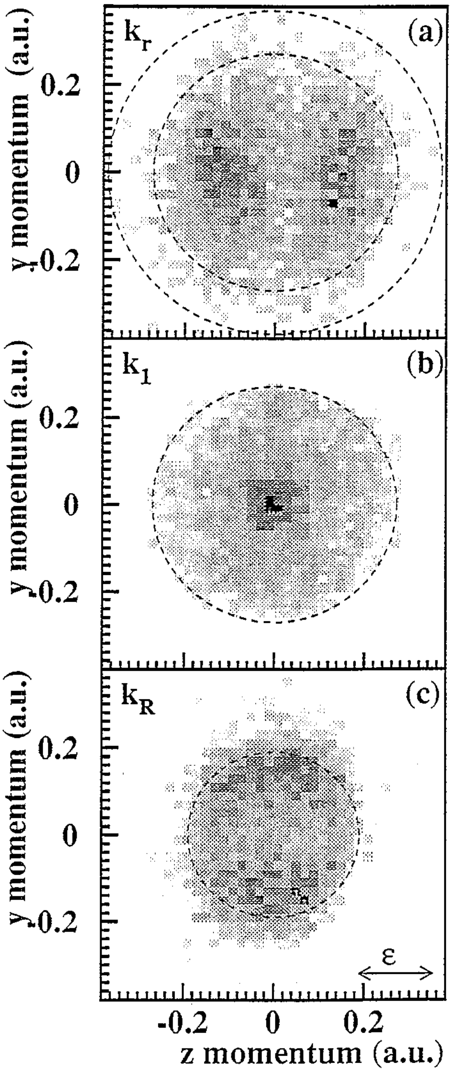

Fig. 4. Momentum distribution after He double ionization 1 eV above the threshold. The z axis is the direction of the polarization vector, the data are integrated over ± 0.1 a.u. in the x direction. (a) Shows the momentum distribution of the recoil ion (k_r, (b) of the electron (k_1 and (c) of $k_R = \frac{1}{2}(k_1 - k_2)$ (from Ref. [22]).

4. Photo double ionization of He close to threshold

Starting with the pioneering work of Schwarzkopf and coworkers in 1993 [27] several groups have reported electron coincidences studies for He double photoionization [28–32]. These experiments have covered several angular settings between the electron spectrometers as well as the cases of equal and unequal sharing of the excess energy available to the system but have been restricted to the coplanar geometry, where the two electrons move in a plane containing the polarization vector of the linear polarized light. As described above the detection of one electron together with the He^{2+} ion yields the same information as the coincident electron detection, however giving 4π solid angle for all fragments. For studies of photoionization this yields a tremendous increase in coincidence count rate. For example, the work by Schwarzkopf [27] reports a coincidence count rate at an excess energy of 20 eV 0.02 Hz. In a recent experiment at the same energy but using COLTRIMS a coincidence rate which was about 4000 times larger has been observed [33].

One of the main advantages of covering the full final state momentum space of all fragments for many particle reactions is that it allows one to display the cross sections not only in coordinates of the particles measured, but in any set of collective coordinates. Depending on the physical process at hand a proper choice of coordinates may reveal in a natural way certain simple characteristics or mechanisms which are hard to see in other coordinates. For the case of He double ionization it has been suggested that at high photon energies which lead to one fast and one slow electron, the single particle momenta are appropriate to the system. At low excess energies the final state interaction between all three particles is known to dominate the momentum distributions. Therefore collective coordinates might be much better adapted to the system. As has been pointed out on several occasions previously, this situation is similar to that encountered in nuclear physics, where the excitation of rotational and vibrational motion is better described in terms of collective rather than single particle coordinates. For the case of He double ionization hyperspherical and Jakobi coordinates have been frequently used for the theoretical description [34,35]. To convert the measured multiple differential cross section into such a set of coordinates, one needs data for all directions and energies of both electrons (and the ion), since the transformation requires an integration over the single particle coordinates (for details see Refs. [36,37]). With the data taken in eventmode with the COLTRIMS setup described above such transformations are straightforward. For each double ionization event one records in an eventmode file the time of flights and the detector positions of one electron and the He^{2+} ion. From this one calculates, event by event, the two electron momenta and the ion momentum (k_1, k_2, k_{ion}) and the Jacobi momenta $k_r = k_1 + k_2 = -k_{ion}$ and $k_R = \frac{1}{2}(k_1 - k_2)$. One can then sort the recorded events with respect to any of those coordinates. If one has recorded a complete set of data at a given photon energy thus any differential cross section can be generated in the offline analysis. As an example Fig. 4 shows the momentum distribution in k_r, k_1 and k_R after double ionization 1 eV above threshold. The light is linear polarized with the polarization vector along the x-axis. The ion is mainly emitted along the direction of polarization, i.e. following the direction of the electric field vector. The distribution looks qualitatively dipole-like reflecting the symmetry imprinted to the system by the photon spin. For the electron (k_1) this dipole pattern is completely washed out by the strong electron–electron interaction of the two slow electrons. This has been already observed by electron spectroscopy [38]. Displaying the data in the k_R momentum space, which is the momentum of the electron not seen from the laboratory, but from the mid-point between the two electrons, again a simple pattern arises. Thus the three particles are arranged in the final state such that the ion emerges preferentially along the electric field vector of the light. The sum momentum of the electron pair has to compensate the ion momentum. The electron pair breaks up along a line perpendicular to the ion momentum. This is in good agreement with what one expects from the Wannier description of the process [35,37]. The measured ion momentum distribution is also found to be in excellent agreement, even in absolute height, with recent a priori calculation by Pont and Shakeshaft [36].

In conclusion, we have illustrated that recoil-ion momentum spectroscopy combined with electron imaging techniques is a unique tool for performing kinematically complete experiments in atomic physics for all possible projectiles like electrons, ions and photons. Although this technique is still very young such complete experiments have already been performed for single and even double ionization by fast highly charged ion impact, [17,19], transfer ionization [10], and the two examples discussed in this paper of slow ion impact and photo double ionization.

Acknowledgements

This work was supported by BMBF, DFG, DAAD, the Max-Planck-Preis and the Feodor Lynen Programm of the Alexander von Humboldt Stiftung, the Studienstiftung des deutschen Volkes, the Division of Chemical Sciences, Office of Basic Energy and by NSF-Int9112815.

References

[1] R. Dörner, T. Vogt, V. Mergel, H. Khemliche, S. Kravis, C.L. Cocke, J. Ullrich, M. Unverzagt, L. Spielberger, M. Damrau, O. Jagutzki, I. Ali, B. Weaver, K. Ullmann, C.C. Hsu, M. Jung, E.P. Kanter, B. Sonntag, M.H. Prior, E. Rotenberg, J. Denlinger, T. Warwick, S.T. Manson and H. Schmidt-Böcking. Phys. Rev. Lett. 76 (1996) 2654.

[2] L. Spielberger, O. Jagutzki, R. Dörner, J. Ullrich, U. Meyer, V. Mergel, M. Unverzagt, M. Damrau, T. Vogt, I. Ali, Kh.

Khayyat, D. Bahr, H.G. Schmidt, R. Frahm and H. Schmidt-Böcking. Phys. Rev. Lett. 74 (1995) 4615.

[3] R. Ali, V. Frohne, C.L. Cocke, M. Stöckli, S. Cheng and M.L.A. Raphaelian. Phys. Rev. Lett 69 (1992) 2491.

[4] V. Mergel, R. Dörner, J. Ullrich, O. Jagutzki, S. Lencinas, S. Nüttgens, L. Spielberger, M. Unverzagt, C.L. Cocke, R.E. Olson, M. Schulz, U. Buck, E. Zanger, W. Theisinger, M. Isser S. Geis and H. Schmidt-Böcking. Phys. Rev. Lett. 74 (1995).

[5] W. Wu, R. Ali, C.L. Cocke, V. Frohne, J.P. Giese, B. Walch, K.L. Wong, R. Dörner, V. Mergel, H. Schmidt-Böcking and W.E. Meyerhof. Phys. Rev. Lett. 72 (1994) 3170.

[6] A. Cassimi, S. Duponchel, X. Flechard, P. Jardin, P. Sortais, D. Hennecart and R.E. Olson. Phys. Rev. Lett. 76 (1996) 3679.

[7] G. Schiwietz. J. Phys. A 37 (1988) 370.

[8] R. Dörner, J. Ullrich, H. Schmidt-Böcking and R.E. Olson. Phys. Rev. Lett. 63 (1989) 147.

[9] A. Gensmantel, J. Ullrich, R. Dörner, R.E. Olson, K. Ullmann, E. Forberich, S. Lencinas and H. Schmidt-Böcking. Phys. Rev. A 45 (1992) 4572.

[10] V. Mergel, Phd Thesis Universität Frankfurt (1996).

[11] G. Brusdeylins, J.P. Toennies and R. Vollmer, title, Publisher, place (Perugia 1989) p. 98.

[12] O. Jagutzki, Dissertation, Unversität Frankfurt (1994).

[13] V. Mergel, Diploma thesis Universität Frankfurt (1994).

[14] R. Dörner, V. Mergel, R. Ali, U. Buck, C.L. Cocke, K. Froschauer, O. Jagutzki, S. Lencinas, W.E. Meyerhof, S. Nüttgens, R.E. Olson, H. Schmidt-Böcking, L. Spielberger, K. Tökesi, J. Ullrich, M. Unverzagt and W. Wu, Phys. Rev. Lett. 72 (1994) 3166.

[15] R. Dörner, V. Mergel, L. Zhaoyuan, J. Ullrich, L. Spielberger, R.E. Olson and H. Schmidt-Böcking, J. Phys. B 28 (1995) 435.

[16] V. Mergel, R. Dörner, J. Ullrich, O. Jagutzki, S. Lencinas, S. Nüttgens, L. Spielberger, M. Unverzagt, C.L. Cocke, R.E. Olson, M. Schulz, U. Buck and H. Schmidt-Böcking, Nucl. Instr. and Meth. 98 (1995).

[17] R. Moshammer, J. Ullrich, M. Unverzagt, V. Schmidt, P. Jardin, R.E. Olson, R. Mann, R. Dörner, V. Mergel, U. Buck and H. Schmidt-Böcking, Phys. Rev. Lett. 73 (1994) 3371.

[18] M. Unverzagt, R. Moshammer, W. Schmitt, R.E. Olson, P. Jardin, V. Mergel, J. Ullrich and H. Schmidt-Böcking, Phys. Rev. Lett. 76 (1996) 1043.

[19] R. Moshammer, J. Ullrich, H. Kollmus, W. Schmidt, R.E. Olson, O. Jagutzki, V. Mergel, H. Schmidt-Böcking, R. Mann and C. Woods, Phys. Rev. Lett. 77 (1996) 1242.

[20] R. Moshammer, M. Unverzagt, W. Schmitt, J. Ullrich and H. Schmidt-Böcking, Nucl. Instr. and Meth. B 108 (1996) 425.

[21] R. Dörner, V. Mergel, L. Spielberger, O. Jagutzki, S. Nüttgens, M. Unverzagt, H. Schmidt-Böcking, J. Ullrich, R.E. Olson, K. Tökesi, W.E. Meyerhof, W. Wu and C.L. Cocke, in: AIP Conf. Proc. 360 (1995), ed. L.J. Dube, J.B.A. Mitchell, J.W. McConckey and C.E. Brion (AIP Press, New York, 1995).

[22] R. Dörner, J. Feagin, C.L. Cocke, O. Jagutzki, M. Jung, E.P. Kanter, H. Khemliche, S. Kravis, V. Mergel, M.H. Prior, H. Schmidt-Böcking, L. Spielberger, J. Ullrich, M. Unverzagt and T. Vogt, Phys. Rev. Lett. 5 (1996) 1025.

[23] R. Dörner, H. Khemliche, M.H. Prior, C.L. Cocke, J.A. Gary, R.E. Olson, V. Mergel, J. Ullrich and H. Schmidt-Böcking, Phys. Rev. Lett. 77 (1996) 4520.

[24] S.D. Kravis, M. Abdallah, C.L. Cocke, C.D. Lin, M. Stöckli, B. Walch, Y. Wang, R.E. Olson, V.D. Rodriguez, W. Wu, M. Pieksma and N. Watanabe, Phys. Rev. A 54 (1996) 1394.

[25] V.D. Rodriguez, Y.D. Wang and C.D. Lin, Phys. Rev. A 52 (1995) R9.

[26] R.E. Olson, Phys. Rev. A 27 (1983) 1871.

[27] O. Schwarzkopf, B. Krässig, J. Elmiger and V. Schmidt, Phys. Rev. Lett. 70 (1993) 3008.

[28] O. Schwarzkopf, B. Krässig, V. Schmidt, F. Maulbetsch and J. Briggs, J. Phys. B 27 (1994) L347-50.

[29] O. Schwarzkopf and V. Schmidt, J. Phys. B 28 (1995) 2847.

[30] A. Huetz, P. Lablanquie, L. Andric, P. Selles and J. Mazeau, J. Phys. B 27 (1994) L13.

[31] P. Lablanquie, J. Mazeau, L. Andric, P. Selles and A. Huetz, Phys. Rev. Lett. 74 (1995) 2192.

[32] G. Dawber, L. Avaldi, A.G. McConkey, H. Rojas M.A. MacDonald, and G.C. King, J. Phys. B 28 (1995) L271.

[33] H. Bräuning, private communication.

[34] J.Z. Tang, S. Watanabe and M. Matsuzawa, Phys. Rev. A 46 (1992) 3758.

[35] J.M. Feagin, J. Phys. B 28 (1995) 1495.

[36] M. Pont and R. Shakeshaft, Phys. Rev. A 51 (1996) R2676.

[37] J.M. Feagin, J. Phys. B (1996) submitted.

[38] R. Wehlitz, F. Heiser, O. Hemmers, B. Langer, A. Menzel and U. Becker, Phys. Rev. Lett. 67 (1991) 3764.